Structure of amorphous $Ge_8Sb_2Te_{11}$: $GeTe$-Sb_2Te_3 alloys and optical storage

J. Akola[1,2,3] and R. O. Jones[1]

[1]*Institut für Festkörperforschung, Forschungszentrum Jülich, D-52425 Jülich, Germany*
[2]*Nanoscience Center, Department of Physics, P.O. Box 35, FI-40014 University of Jyväskylä, Finland*
[3]*Department of Physics, Tampere University of Technology, P.O. Box 692, FI-33101 Tampere, Finland*

The amorphous structure of $Ge_8Sb_2Te_{11}$, an alloy used in the Blu-ray Disc, the *de facto* successor to digital versatile disk (DVD) optical storage, has been characterized by large-scale (630 atoms, 0.4 ns) density-functional/molecular-dynamics simulations using the new PBEsol approximation for the exchange-correlation energy functional. The geometry and electronic structure agree well with available x-ray diffraction data and photoelectron measurements. The total coordination numbers are Ge: 4.0, Sb: 3.7, and Te: 2.9, and the Ge-Ge partial coordination number is 0.7. Most atoms (particularly Sb) prefer octahedral coordination but 42% of Ge atoms are "tetrahedral." Structural details, including ring statistics, local coordination, and cavities (12% of total volume), are strikingly similar to those of $Ge_2Sb_2Te_5$, which is used in DVD–random access memory. The presence of less than 10% Sb atoms leads to significant changes from GeTe.

I. INTRODUCTION

Recording layers of contemporary digital versatile disk (DVD) media [DVD-random access memory (RAM), DVD-rewritable (RW), and Blu-ray Disc (BD)] are based on phase-change materials (PCMs), which utilize rapid and reversible transitions between the amorphous and crystalline phases of nanosized spots on a polycrystalline film. Differences between the optical contrast and electrical resistivity of the two phases allow one to identify the state. In practice, data are recorded by applying a short and intense laser pulse (set pulse of ~ 1 ns) that melts the film locally. Subsequent rapid cooling (melt quench) results in an amorphous bit (diameter of ~ 10–100 nm), which can be erased (reset) by heating above the glass transition temperature using a weaker pulse (some tens of ns). PCM are prime candidates for nonvolatile computer memories of the future (phase-change random access memory),[1] as they have fewer problems at nanometer length scales than the other main contender, flash memory. Prototype devices based on PCM technology enable data-storage densities of the order of 1 Tbit cm^{-2}.[2]

Many crystalline materials amorphize rapidly but the need for rapid recrystallization eliminates most of them for optical storage purposes. Many successful PCM alloys are (a) pseudobinary alloys of the form $(GeTe)_{1-x}(Sb_2Te_3)_x$ (GST materials) or (b) doped SbTe alloys near the eutectic composition $Sb_{70}Te_{30}$. The former include some of the best known, including the DVD-RAM material $Ge_2Sb_2Te_5$ (GST-225, $x=\frac{1}{3}$).[3] GST-225 shows good phase-change behavior but the reduction in the thickness of the recording film (to 6–10 nm) has been accompanied by amorphous bit instability and the optical contrast for BD applications (blue-violet laser, 405 nm) is not ideal. GeTe-rich alloys with small values of x are better and it has been found that the optical contrast between the two phases increases monotonically as $x \rightarrow 0$.[4] On the other hand, it has been known for many years that the most rapid crystallization occurs for larger values of x, as in $GeSb_4Te_7$ ($x=\frac{2}{3}$). Compromises are necessary, and $Ge_8Sb_2Te_{11}$ (GST-8,2,11, $x=\frac{1}{9}$) is a material of choice for BD.[4]

The amorphous-crystalline phase change cannot be understood without knowing the structures involved. The *crystalline* phases of GeTe-rich alloys in the family $[(GeTe)_{1-x}(Sb_2Te_3)_x, x \leq \frac{1}{3}]$ have been studied for many years. In most cases there is a metastable phase with a distorted NaCl structure and a higher temperature phase with homologous structures.[4] Vacancies play an essential role in stabilizing the NaCl structure over a wide range of x.[5] Density-functional calculations have been performed for crystalline structures with compositions $(GeTe)_{1-x}(Sb_2Te_3)_x$ and nearby stoichiometries.[6,7] The most recent calculations $[Ge_3Sb_2Te_6, Ge_2Sb_2Te_5, GeSb_2Te_4,$ and $GeSb_4Te_7$ ($x=\frac{1}{4}, \frac{1}{3}, \frac{1}{2},$ and $\frac{2}{3}$, respectively)] suggest that the stability of these compounds is enhanced by maximizing the number of Te atoms surrounded by three Ge and three Sb atoms.[7] The *amorphous* structures of chalcogenide alloys remain a challenging problem for experimentalists and theorists. Scattering methods provide much less structural information than in crystals with long-range order, although extended x-ray absorption fine structure (EXAFS) provides details of the local coordination and bond lengths. It is astonishing that almost nothing is known about the amorphous structure of GST-8,2,11, a material now used for the third generation optical storage, BD.[4] Until very recently, this observation applied to the amorphous phases of almost *all* PCMs.

Experimental work on binary Ge_xTe_{1-x} alloys[8–10] and GST-225 (Refs. 11–14) has given rise to speculations concerning their structural phase changes. In GST-225, for example, it has been proposed that a Ge atom flips between tetrahedral and octahedral sites.[11] Recent numerical simulations of the amorphous phases[15–19] have provided new information and a more consistent picture of both systems: (a) octahedral bond angles predominate,[12,15,17,19] (b) tetrahedrally coordinated Ge atoms do occur,[15,17,19] (c) even-numbered rings are characteristic,[12] particularly "*ABAB* squares" (*A*: Sb, Ge; *B*: Te),[15,18,19] and (d) Te atoms (and Sb in GST-225) are overcoordinated; i.e., they do not obey the "$8-N$" rule, where N is the number of valence electrons.[13,15,17,19] One might speculate that GST-8,2,11 has

similar features to GST-225, or that its GeTe-rich nature ($x=\frac{1}{9}$) could lead to a close resemblance to GeTe ($x=0$). We show that the first assumption is valid but the latter is not. Structural details in amorphous GST-8,2,11 are very similar to GST-225, indicating that the addition of only a few percent of Sb changes the properties of GeTe significantly.

The density-functional (DF) method is free of adjustable parameters and has well-established predictive value in many contexts, including chalcogenide materials.[20] In combination with molecular dynamics (MD), it is ideal to study amorphous (a-) and liquid (ℓ-) PCM. However, the computational demands are such that they are often restricted to short simulations of small systems. Recently, we reported DF calculations of GST-225 with 460 atoms in the unit cell over hundreds of picoseconds.[15,16] Such times approach the experimental quenching time (~ 1 ns) and proved to be essential to describe the ordering correctly. Simulations of amorphous (i.e., disordered) materials require large systems (several hundred atoms) to provide adequate statistics for each element and to minimize artificial long-range order that periodic boundary conditions can induce. We apply this approach here for GST-8,2,11 (630 atoms) in a simulation of over 400 ps and compare the results with those for GeTe and GST-225.

II. METHOD OF CALCULATION

We have used the CPMD program,[21] as in our earlier work on GST alloys[15,16,19] but we have adopted here the recent PBEsol approximation[22] for the exchange-correlation energy. This has the same analytic form as that of Perdew-Burke-Ernzerhof (PBE) (Ref. [23]) used previously but two parameters ($\mu = 10/81 \approx 0.1235$ and $\beta = 0.046$) have been adjusted to describe better the equilibrium properties of densely packed solids. The new form gives better lattice constants and surface energies than PBE calculations, which overestimate bond lengths in GST materials.[15,16,19] Both forms are compatible with the scalar-relativistic pseudopotentials we use for the electron-ion interactions.[24] We use periodic boundary conditions with a single point ($\mathbf{k}=0$) in the Brillouin zone, a kinetic-energy cutoff for the plane wave basis of 20 Ry,[25] and Born-Oppenheimer (BO) MD with a Nosé-Hoover thermostat (frequency of 800 cm^{-1} and chain length of 4).[26] BO MD uses an efficient predictor-corrector algorithm that allows time steps for initialization [250 a.u. (6.050 fs)] and data collection [125 a.u. (3.025 fs)] that are much longer than are possible using Car-Parrinello dynamics. This advantage outweighs the larger computational cost per time step (between 10 and 20 iterations are required to reoptimize the wave function at each geometry), and the present approach is stable even when the band gap at the Fermi energy is small or vanishes, as in liquid GST-8,2,11. Car-Parrinello simulations do not guarantee separation of the electronic and ionic degrees of freedom in such systems and are less appropriate for the study of melt-quench processes.

We simulate 630 atoms (240 Ge, 60 Sb, and 330 Te, the exact composition of GST-8,2,11) in a cubic cell of dimension (27.19 Å) appropriate to the liquid density (0.031 34 atoms/Å^3).[27] The starting geometry was based in
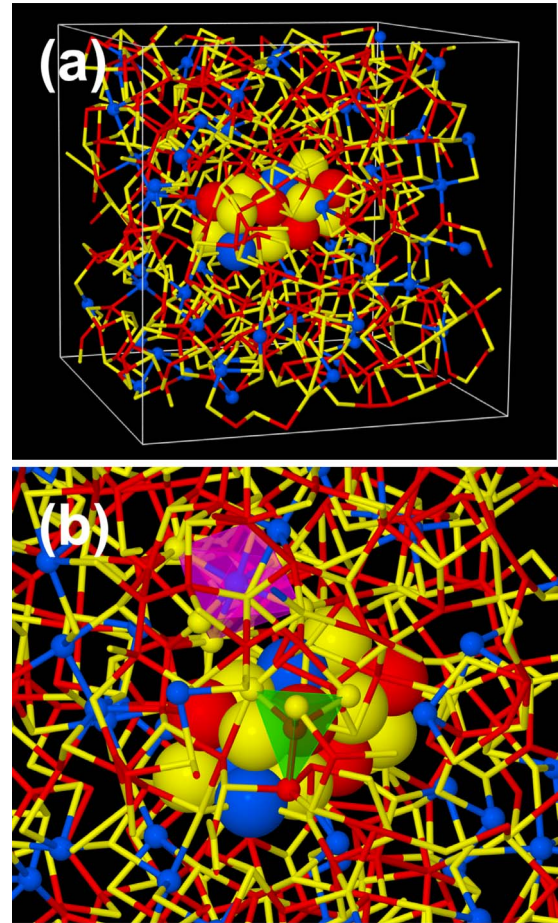

FIG. 1. (Color online) (a) Simulation box of a-GST-8,2,11 (27.06 Å, 630 atoms). A "column" showing AB ordering is shown and Sb atoms are highlighted with small spheres. Red (light gray): Ge; yellow (white): Te; blue (dark gray): Sb. (b) Structure with tetrahedrally coordinated Ge atom shown in green, octahedrally coordinated Sb in pink.

part on our optimized geometry for a-GST-225 (460 atoms).[15] After heating to 3000 K, the sample was cooled (120 ps) to the melting point (950 K), where data were collected (31 ps). During subsequent cooling to 300 K (melt quench, 217 ps), there was a (small) adjustment of the density to that of the amorphous material (0.031 79 atoms/Å^3 and cell dimension of 27.06 Å).[28] This was followed by a data collection (30 ps) and cooling to 100 K (31 ps), where the structure was optimized by simulated annealing. The total simulation time of the melt-quench process was 429 ps. The optimized structure [Fig. 1(a)] shows a cubic column of 16 atoms that demonstrates AB ordering, and Fig. 1(b) emphasizes the local coordination of Ge and Sb atoms. Information derived from the structure is given in Table I and will be discussed in Sec. III. More details of the methods of calculation and analysis are provided in Ref. 15.

We have also performed calculations for a *crystalline* sample of 611 atoms in an orthorhombic cell of dimension $30.09 \times 24.07 \times 24.07$ Å^3.[29] Based on the rocksalt geometry with 640 atomic sites, 320 Te atoms populate Cl sites, and Ge (233), Sb (58 atoms), and vacancies (29 sites) occupy Na sites randomly, as proposed by Yamada[3] for GST materials.

TABLE I. Calculated properties of a-$(GeTe)_{1-x}(Sb_2Te_3)_x$ alloys. r_{X-Y}: position of first maximum in PDF, $n(X)$: total coordination number, n_{X-Y}: partial coordination number of Y atoms surrounding X atoms (n_{Y-X} in parentheses), V_c: total cavity volume, $\langle v \rangle$: average cavity size, and E_g: electronic band gap. The coordination numbers have been calculated by applying a bond cutoff distance of 3.2 Å.

Alloy	GeTe[a]	GST-8,2,11	GST-225[a]
x	0	1/9	1/3
r_{Ge-Te} (Å)	2.78	2.73	2.78
r_{Ge-Ge} (Å)	2.60	2.54	2.84
r_{Ge-Sb} (Å)		2.75	2.79
r_{Sb-Te} (Å)		2.88	2.93
r_{Sb-Sb} (Å)		2.92	2.96
r_{Te-Te} (Å)	2.87	2.85	2.95
$n(Ge)$	4.2	4.0	4.2
$n(Sb)$		3.7	3.7
$n(Te)$	3.3	2.9	2.9
n_{Ge-Te}	3.2	3.2 (2.3)	3.6 (1.4)
n_{Ge-Ge}	1.1	0.7	0.4
n_{Ge-Sb}		0.2 (0.6)	0.2
n_{Sb-Te}		2.8 (0.5)	2.9 (1.2)
n_{Sb-Sb}		0.2	0.6
n_{Te-Te}	0.1	0.1	0.3
V_c (%)	6.4	12.4	11.7
$\langle v \rangle$ (Å^3)	40.9	51.6	54.2
E_g (eV)	0.13	0.31	0.19

[a]PBE functional (Refs. 15 and 16).

Structural optimization of this geometry results in splitting of both Ge-Te and Sb-Te bonds to shorter and longer bonds. The PBEsol bond lengths (Ge-Te: 2.86/3.13 and Sb-Te: 2.98/3.19 Å) are in excellent agreement with the x-ray diffraction measurements of crystalline GST-8,2,11. These measurements do not distinguish between Ge-Te and Sb-Te bonds and give 2.88 and 3.10 Å for the shorter and longer bonds, most of which are Ge-Te.[4] These values are 1%–2% shorter than the PBE results for GST-225. The calculated cohesive energy of crystalline GST-8,2,11 is 3.02 eV, and the melt-quenched amorphous sample is 0.084 eV/atom higher in energy.

III. RESULTS

A. Structures

The optimized structure of a-GST-8,2,11 leads immediately to the pair distribution function (PDF) $g(r)$ [Fig. 2(b)], and Fourier transformation (with weights appropriate for x-ray scattering)[15] yields the structure factor $S(Q)$ [Fig. 2(a)]. We know of no published scattering data for this material but a comparison of the present results with the measurements on GeTe and GST-225 (Ref. 12) [Figs. 2(a) and 2(b)] is instructive. The calculation shows peaks at 2.0, 3.3, and 4.9 Å^{-1}. In particular, the calculated $g(r)$ and $S(Q)$ for GST-8,2,11 are closer to the measured value for GST-225 than to
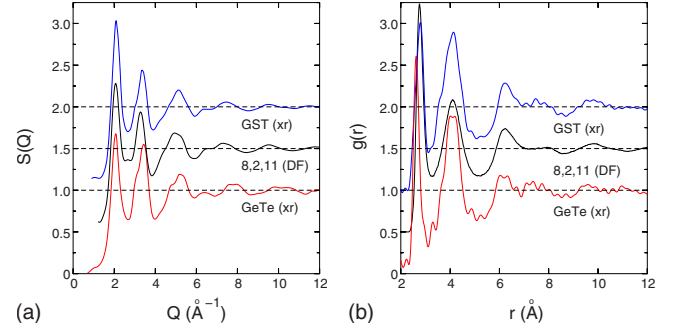

FIG. 2. (Color online) (a) Structure factor $S(Q)$ and (b) XRD-weighted total pair distribution function $g(r)$. The experimental results are from Ref. 12.

those of GeTe. This impression is supported by the comparison of the calculations for all three alloys, which is provided as Supplementary Information.[30]

The six partial PDF are shown in Fig. 3 for the liquid (950 K) and amorphous (300 K) phases, and numerical values for the amorphous phase are given in Table I. There are clear similarities with our previous studies on other alloys:[15,16,19] Ge-Te and Sb-Te bonds dominate with partial coordination numbers of 3.2 and 2.8, respectively, Te-Te PDF shows medium-range oscillations that extend beyond 10 Å, and the number of "wrong bonds" (i.e., bonds not occurring in the crystal) is much lower after quenching. The usage of PBEsol functional reduces bond lengths by 1%–2%, and the values of 2.54, 2.73, and 2.88 Å for Ge-Ge, Ge-Te, and Sb-Te bonds are closer to the EXAFS results (2.48, 2.63, and 2.85 Å) for GST-225.[13] As in a-GST-225,[15,16] both Sb and Te have higher coordination than expected from the "$8-N$ rule," where N is the number of valence electrons. The Ge-Ge coordination number (0.7) is significantly less than in GeTe.

Sb shows details that are particularly interesting. As in other GST alloys, the Sb-Te PDF has a strong first peak that
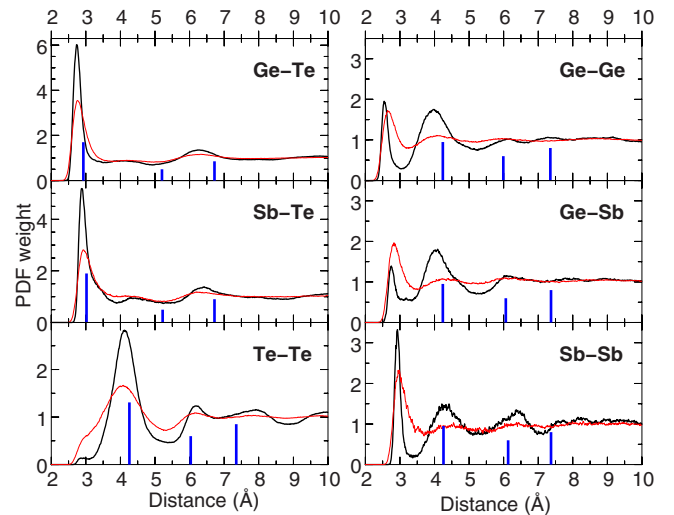

FIG. 3. (Color online) Calculated partial pair distribution functions in GST-8,2,11: thick black: 300 K and red (gray): 950 K. The blue vertical bars correspond to the optimized crystalline sample of GST-8,2,11.
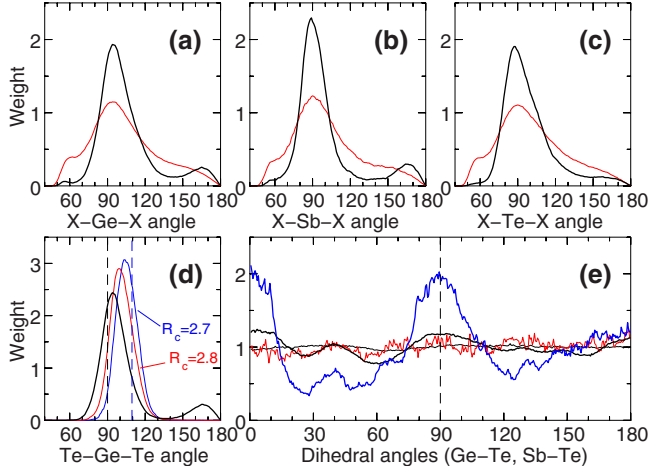
FIG. 4. (Color online) [(a)–(d)] Bond angle distributions in GST-8,2,11: black: 300 K and red (gray): 950 K. (d) shows the dependence on cutoff R_c (in Å) at 300 K. Vertical dashed lines mark octahedral and tetrahedral angles. (e) Dihedral angle distributions for -Ge-Te- (thick black: 300 K and thin black: 950 K) and -Sb-Te- (blue, strongly varying curve): 300 K and red (gray): 950 K.

decays slowly (minimum at 3.9 Å) but the Sb-Sb PDF reveals short-to-medium-range correlation among the sparsely distributed Sb atoms [see Fig. 1(a)]. The number of Sb-Sb bonds (0.2 per Sb) does not reduce upon quenching but the corresponding first PDF peak becomes very sharp at 2.92 Å. There are pronounced maxima at 4.3 and 6.4 Å and a final minimum at 7.0 Å.

Figure 4 shows the bond angle distributions for Ge, Sb, and Te, as well as the distributions of dihedral angles around Ge-Te and Sb-Te bonds. A bond cutoff distance of 3.2 Å has been used. All three elements [Figs. 4(a)–4(c)] prefer angles of 90°, and Ge and Sb also favor linear configurations of 180°. As found in GST-225,[15,16] the maximum in Ge (94°) is shifted slightly, and Fig. 4(d) shows that a shorter bond cutoff moves the maximum closer to the tetrahedral value (109.47°), indicating tetrahedrally coordinated Ge atoms. The coordination in Sb, by contrast, is definitely octahedral. The effect of high temperature (liquid, 950 K) is visible as overall broadening of the distributions, and the maxima at 60° correspond to triangular configurations (rings, see below).

The dihedral angle distributions in Fig. 4(e) are particularly interesting: At 300 K, Ge shows some preference for octahedral angles (0°, 90°, and 180°) but the greatly enhanced maxima for Sb at 0° and 90° (not 180°) support the picture of octahedral bond angles. In spite of there being relatively few Sb-Te bonds, they enhance the occurrence of square and cubic arrangements. This effect is more pronounced in GST-8,2,11 than in GST-225 (Refs. 15 and 16) and also explains the Sb-Sb oscillations in the PDF (Fig. 3).

The local order of atomic types (*A*: Ge, Sb; *B*: Te) can be quantified by order parameters that consider both *AB* alternation and bond angles.[16] The contribution of atom *i* of type *A* is
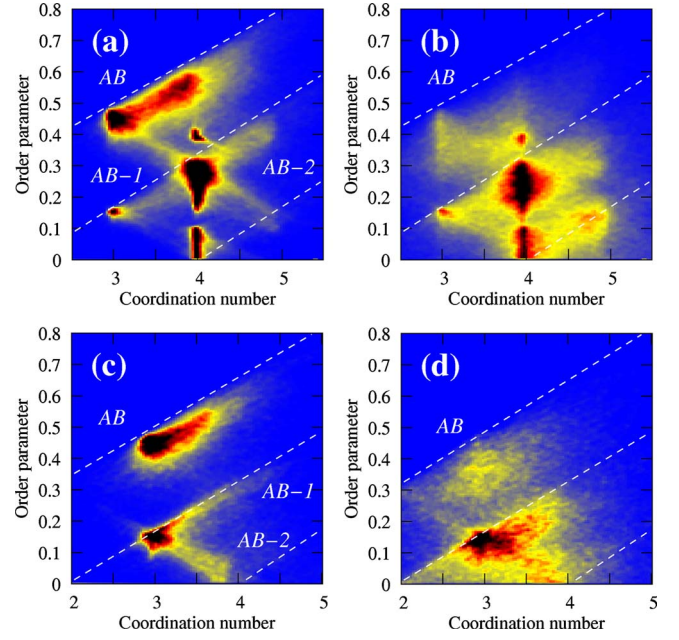

FIG. 5. (Color online) Local order-parameter maps in $Ge_8Sb_2Te_{11}$: amorphous [300 K; (a) Ge and (c) Sb] and liquid [950 K; (b) Ge and (d) Sb] phases. The diagonal dashed lines mark octahedral bond angles for a given degree of *AB* alternation.

$$\alpha_i^{(A)} = \frac{1}{n_B} \sum_{j \neq i} f(r_{ij}) \frac{\sum_{k \neq i,j} |f(r_{ik})| g(\theta_{ijk})}{\sum_{k \neq i,j} |f(r_{ik})|}, \qquad (1)$$

where n_B is the number of nearest neighbors in the rocksalt structure (6, type *B*). A similar formula holds for type *B* (Te) atoms. The sign of $f(r_{ij})$, the cutoff distance for counting nearest neighbors, depends on bond type (positive for *AB* bonds, negative otherwise):

$$f(r_{ij}) = \frac{\pm 1}{\exp[\kappa^{-1}(r_{ij} - r_0)] - 1}, \qquad (2)$$

and $g(\theta_{ijk})$ is the angular weighting function:

$$g(\theta_{ijk}) = \cos^2[2(\theta_{ijk} - \theta_0)]. \qquad (3)$$

The order parameter is unity for crystalline phases of GST alloys with *AB* alternation, and it vanishes for complete disorder. The parameters ($r_0 = 3.2$ Å, $\kappa = 0.05$ Å, $\theta_0 = 90°$) are the same as in Ref. 16.

The color maps of $\alpha_i^{(A)}$ for Ge and Sb (Fig. 5) show clear differences between Ge and Sb and between the amorphous and liquid phases. At 300 K, Sb atoms [Fig. 5(c)] prefer octahedral bond angles (dashed lines) and coordination between 3 and 4, while Ge [Fig. 5(a)] includes maxima [(4,0.4), (4,0.2), and (4,0.1)] corresponding to tetrahedral bond angles [see Fig. 4(d)]. Integration over these areas shows that 42% of Ge atoms have tetrahedral coordination in *a*-GST-8,2,11 at 300 K.[31] This is consistent with our results on *a*-GST-225 and *a*-GeTe but we note that GeTe-rich alloys have larger concentrations of tetrahedral Ge. Among many local configurations, the most common include Ge-GeTe₃
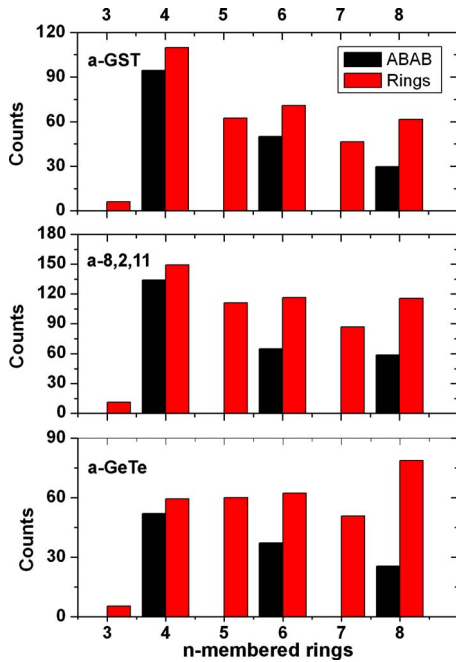
FIG. 6. (Color online) Statistics of irreducible rings (300 K) in Ge$_2$Sb$_2$Te$_5$, Ge$_8$Sb$_2$Te$_{11}$, and GeTe alloys. *ABAB* configurations refer to alternation of atomic type *A* (Ge, Sb) and B (Te). The bond cutoff distance is 3.2 Å. The results for Ge$_2$Sb$_2$Te$_5$ and GeTe are from Ref. 15.

(23% of Ge atoms), Sb-Te$_3$ (26% of Sb), and Te-Ge$_3$ (33% of Te). The increased disorder of the liquid is reflected in the range of configurations [Figs. 5(b) and 5(d)] but $\alpha_i^{(A)}$ tends to be positive. In the liquid (950 K), the weight of threefold coordinated Ge is less, there are more Ge atoms with higher coordination, and tetrahedral Ge atoms are also prevalent (32%).

The ring statistics of amorphous Ge$_8$Sb$_2$Te$_{11}$, GeTe, and GST-225 are compared in Fig. 6. There are many four-membered rings and few triangular configurations in all cases. As in GST-225, most of the four-membered rings in Ge$_8$Sb$_2$Te$_{11}$ show *AB* alternation, confirming that the basic building blocks in the amorphous and crystalline (rocksalt) phases are *ABAB* squares.[15,17,18] A good example is the *ABAB* column shown in Fig. 1. The odd-even alternation is apparent in GST-8,2,11 and GST-225, and the ring distributions of these two materials are strikingly similar. This may be surprising at first since GST-8,2,11 is much closer to GeTe on the pseudobinary line but even a small amount of Sb ($x = \frac{1}{9}$) appears to change the properties of GeTe significantly.

In the metastable crystalline phase, (GeTe)$_{1-x}$(Sb$_2$Te$_3$)$_x$ materials contain intrinsic vacancies on Na sites whose concentration varies as $x/(1+2x)$.[5] Empty space (cavities, voids) also occurs in the amorphous phase and is essential for the phase change to occur without forcing many bonds to break and reform. We noted previously that the higher vacancy concentration in GST-225 (11.7%, see Table I) than in GeTe (6.4%) is consistent with its improved performance as a phase change material.[15] The method we use to define and analyze cavities is described in detail in Ref. 15.
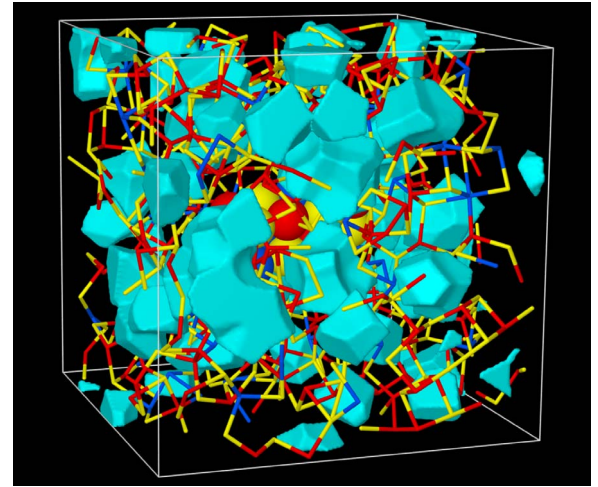

FIG. 7. (Color online) Cavities in melt-quenched GST-8,2,11. The volumes have been constructed around regions at least 2.8 Å from any atom.

Cavity shapes include facets, edges, corners, and protrusions. They are illustrated in Fig. 7 for the optimized structure of *a*-GST-8,2,11, where they occupy 12.4% of the total volume; i.e., the increase in x from 0 to $\frac{1}{9}$ is accompanied by a dramatic increase in the number of cavities to a value near that in *a*-GST-225. The coordination numbers around the vacancy centers are 1.3, 0.4, 3.7, and 0.2 for Ge, Sb, Te, and other vacancies, respectively. The atom-cavity PDF are given in the Supplementary Information.[30] The cavities are then surrounded mainly by Te atoms, and Ge is a more common neighbor than Sb. These features reflect the small Sb content and the underlying cubic structure that resembles the crystalline phase.

The charges inside the cavities calculated using the Voronoi construction lie between 1 and 5 electrons, with an average value of 2.0. As found in GST-225, the charge arises from lone pair orbitals of neighboring Te atoms at the edges of the cavities and there is no charge at the cavity centers. The average vacancy in the *crystalline* phase contains 1.6 electrons, close to the amorphous value. The larger volume fraction (19.3%) occupied by cavities in *liquid* GST-8,2,11 (950 K) is consistent with the increased coordination number of Ge (4.3) and reduced density. The average cavity volume in the liquid (62.7 Å^3) is somewhat higher than that in the amorphous system at 300 K (51.6 Å^3).

B. Electronic structure

The electronic density of states (DOS) of amorphous and crystalline phases of Ge$_8$Sb$_2$Te$_{11}$ are compared with hard x-ray photoemission spectra (XPS) (Ref. 14) in Fig. 8(a). Both phases show band gaps (0.31 and 0.45 eV) and the overall agreement between theory and experiment is very good. The semiconducting nature of *c*-GST-8,2,11 is closely related to the presence of vacancies on Na sites, which help stabilize the rocksalt structure [the p^3-bonded structure must include 6N(Te) p electrons].[5,15] Deviations from the pseudobinary tie line shift the band gap and change conductivity and optical reflectivity.[1]
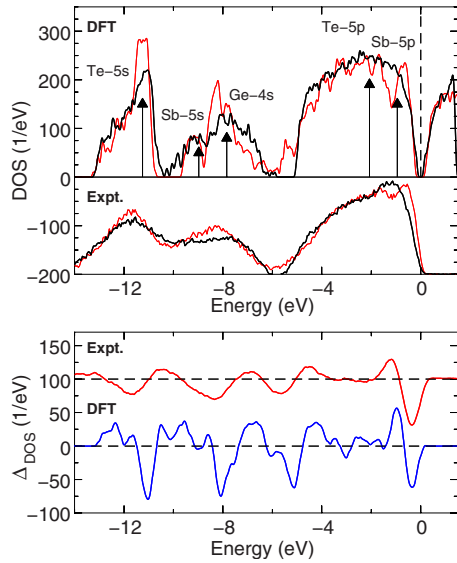
FIG. 8. (Color online) (a) Electronic DOS of amorphous (thick black curve) and crystalline [red (gray) curve] $Ge_8Sb_2Te_{11}$ compared with the XPS measurements of Ref. 14 (lower curves). Atomic eigenvalues are also shown by shifting the Ge $4p$ orbital energy at the Fermi level. (b) DOS difference between the amorphous and crystalline alloys.

The overall shapes of the DOS profiles display a three-band-structure characteristic of materials with average valence near 5 (5.14 for GST-8,2,11). The first two (σ) bands can be assigned to s electrons [the arrows in Fig. 8(a) are the energy eigenvalues of the atoms], and the broad valence ($\pi-$) band up to the Fermi level has p character. The band gaps near -10 and -6 eV differ in the two phases. The former is reduced in the amorphous phase by the increased s-s interaction between Sb and Te, while the latter increases. Moreover, the calculated *difference* between the DOS of the two phases agrees very well with experiment, particularly near the Fermi energy, so that the optimized amorphous structure reproduces the reported change in the electronic properties. The atomic projections of the DOS for a- and c-GST-8,2,11 are shown in Supplementary Figure 3. The former are very similar to those in a-GST-225 (Ref. 16) and to the DOS at 950 K. We note, however, the d contribution on Sb and Te sites in the present calculations. As in GST-225, the DOS for the liquid phase has no gap at the Fermi energy.

These findings provide insight into the experimental results. First, the XPS measurements[14] reveal a systematic positive shift of the Sb $4d$ core-level spectrum in the $(GeTe)_{1-x}(Sb_2Te_3)_x$ alloys, including $x=\frac{1}{9}$. This effect vanishes for very small Sb concentrations and is probably related to the increased Sb-Te interaction in the amorphous phase that eliminates the band gap at -10 eV. Second, GeTe-rich alloys show larger changes in electronic and optical properties that correlate with the increasing concentration of tetrahedral sp^3-bonded Ge atoms in these materials.[32] For a-GST-8,2,11, 42% of Ge atoms belong to this category so that 16% of *all atoms* are not bound octahedrally (p^3). This should increase further for $x<\frac{1}{9}$.

Finally, we have calculated the effective charges of the elements in both amorphous and crystalline phases using the
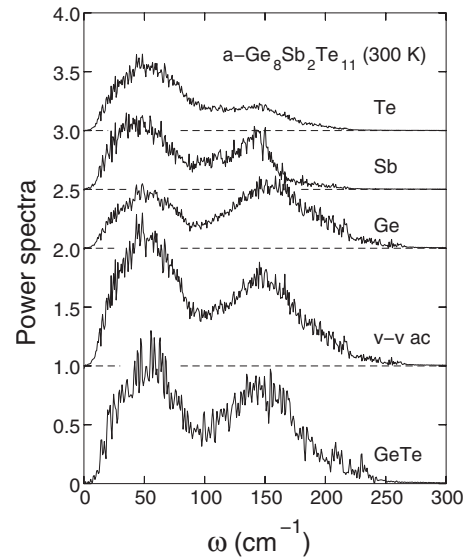

FIG. 9. Power spectra of a-GeTe and a-GST-8,2,11 (vv-ac, maximum values of 1.3) at 300 K and projections onto Ge, Sb, and Te atoms (maximum values of 0.65).

Voronoi prescription. In the former, Ge sites have a maximum value of -0.16 electrons (average value of -0.18), Sb 0.24 (0.24), and Te 0.13 (0.09). In the crystalline phase the corresponding values are Ge -0.11 electrons (-0.18), Sb 0.31 (0.21), and Te 0.22 (0.10). The corresponding charge distributions are shown in Supplementary Figure 4. Sb is the most cationic element, as confirmed by calculations of Mulliken and Löwdin charges. There are again similarities to the results we found in a-GST-225, although we note that the present simulations are longer, study a larger number of atoms, and use the PBEsol functional form instead of PBE.

C. Dynamical properties

Vibration frequencies provide a valuable means of structure determination in many contexts, and the frequency spectrum for a-GST-8,2,11 at 300 K (Fig. 9) has been determined from the Fourier transformation of the velocity-velocity autocorrelation function obtained from a trajectory of 10 000 time steps of 3.025 fs each. Each frequency has been broadened with a Gaussian of width of 1 cm^{-1}. Also shown is the power spectrum of GeTe from a trajectory of 8700 time steps of the same length. As in GST-225,[16] there are broad peaks near 60 and 150 cm^{-1} and a tail above 180 cm^{-1}. The tails that extend up to 250 cm^{-1} arise mainly from vibrations of the lightest element Ge, particularly of atoms with fourfold coordination and Ge-Ge bonds. The narrow Sb projection maximum at 150 cm^{-1} is related to the limited range of local (distorted octahedral) configurations.

The calculated atomic mean-square displacements of the liquid alloy shows a linear dependence on time, and the diffusion constants are $D_{Ge}=5.20\times10^{-5}$, $D_{Sb}=5.57\times10^{-5}$, and $D_{Te}=4.24\times10^{-5}$ cm^2 s^{-1} at 950 K. These values are higher than in GST-225 (Ge: 3.93, Sb: 4.67, and Te: 3.78) and GeTe (Ge: 4.65 and Te: 3.93),[15] reflecting in part the higher melting point (compared to former) and the volume of cavities

(latter). As in the case of GST-225,[15] Sb is the most mobile element but the difference between Ge and Sb is lower. Viscosity estimates depend on the particle radius in the Stokes-Einstein relation, and a plausible value (1.4 Å) leads to 1.1 cP. The measured value of ℓ-GeTe ranges from 1.9 and 1.2 cP between 1000 and 1200 K.[33]

IV. DISCUSSION

The pseudobinary alloys $(GeTe)_{1-x}(Sb_2Te_3)_x$ have been at the forefront of research and development of phase-change memory materials for the past two decades. $Ge_2Sb_2Te_5$ ($x=\frac{1}{3}$) is the prototype and best studied of these materials but GeTe-rich compositions have been found to possess several advantages. $Ge_8Sb_2Te_{11}$ ($x=\frac{1}{9}$) and alloys with even smaller values of x are now used as recording media in the BD, the *de facto* successor to the DVD as the omnipresent optical storage.

Important experimental studies on this family of materials include x-ray diffraction studies of 17 crystalline specimens from GeTe ($x=0$) to GeSb$_4$Te$_7$ ($x=\frac{2}{3}$).[4,5] At room temperature, samples with $0 \le x \le \frac{1}{3}$ crystallize into a deformed NaCl (rhombohedral) structure and the remainder into an NaCl (cubic) phase. The NaCl structures are stabilized by vacancies that increase in number as x increases. High-energy x-ray photoelectron spectroscopy for eight alloys with $0 \le x \le \frac{1}{3}$ provide valuable information about the valence-band densities of states of crystalline and amorphous materials (and their differences).[14]

Our earlier DF/MD simulations on GeTe and Ge$_2$Sb$_2$Te$_5$ (Refs. 15, 16, and 19) agreed very well with measured structure factors[12] and have been extended here to a melt-quench simulation of Ge$_8$Sb$_2$Te$_{11}$. The sample size (630 atoms) reduces the effect of periodic boundary conditions and generates adequate statistics for atoms and cavities, and the simulation time (more than 0.4 ns) represents reliably the experimental procedure used to produce the amorphous phase and accommodates the structural relaxation (e.g., "wrong bonds") that arises during rapid cooling. The use of an improved exchange-correlation functional, PBEsol, results in shorter bond lengths and improved agreement with experiment for both the crystalline and amorphous phases. Our aim has been to identify and compare crucial elements in the structural properties of these materials.

The properties of GST-225 and GST-8,2,11 are strikingly similar. The Te-Te and Sb-Sb pair-correlation functions show medium range order, and the dihedral angle distributions show that cubic arrangements of Te and, in particular, Sb atoms are favored. The Sb coordination can also be described as "distorted octahedral"[17] or "Peierls distorted"[34] since the integration of the Sb-Te PDF up to the first minimum (3.9 Å) gives a total coordination number close to 6. XPS measurements of the valence electron densities of states in GST-225 and GST-8,2,11 are reproduced well in both amorphous and crystalline forms, as are the differences between the two phases. The ring distributions in the amorphous phases of these two materials are very similar, particularly the *ABAB* rings (*A*: Ge, Sb; *B*: Te) that are crucial to the rapid phase change. The volumes occupied by vacancies in amorphous GST-225 (11.7%) and GST-8,2,11 (12.4%) are also very similar. We have noted[15,16] the importance of the cavities in providing free space for the atomic rearrangement involved in the phase change.

The differences between a-GST-225 and a-GST-8,2,11 are small but significant: the latter has a larger Ge-Ge coordination number and a larger fraction of Ge atoms with tetrahedral coordination. By contrast, GeTe differs from both GST-225 and GST-8,2,11 in its ring distribution, the increased number of Ge-Ge bonds, and the much lower vacancy volume (6.4%). Our calculations indicate that GeTe is indeed a special case in this family of materials, and that even a small addition of Sb atoms (9% in GST-8,2,11) suffices to give structural properties very similar to the prototype GST-225.

[1] M. Wuttig and N. Yamada, Nat. Mater. **6**, 824 (2007) and references therein.

[2] H. F. Hamann, M. O'Boyle, Y. C. Martin, M. Rooks, and H. K. Wickramasinghe, Nat. Mater. **5**, 383 (2006).

[3] N. Yamada, Mat. Res. Soc. Bull. **21**, 48 (1996).

[4] T. Matsunaga, H. Morita, R. Kojima, N. Yamada, K. Kifune, Y. Kubota, Y. Tabata, J.-J. Kim, M. Kobata, E. Ikenaga, and K. Kobayashi, J. Appl. Phys. **103**, 093511 (2008).

[5] T. Matsunaga, R. Kojima, N. Yamada, K. Kifune, Y. Kubota, Y. Tabata, and M. Takata, Inorg. Chem. **45**, 2235 (2006).

[6] J. H. Eom, Y. G. Yoon, C. Park, H. Lee, J. Im, D. S. Suh, J. S. Noh, Y. Khang, and J. Ihm, Phys. Rev. B **73**, 214202 (2006).

[7] J. L. F. Da Silva, A. Walsh, and H. Lee, Phys. Rev. B **78**, 224111 (2008).

[8] Y. Maeda and M. Wakagi, Jpn. J. Appl. Phys., Part 1 **30**, 101 (1991).

[9] J. Y. Raty, V. V. Godlevsky, J. P. Gaspard, C. Bichara, M. Bionducci, R. Bellissent, R. Céolin, J. R. Chelikowsky, and P. Ghosez, Phys. Rev. B **65**, 115205 (2002).

[10] A. V. Kolobov, P. Fons, J. Tominaga, A. L. Ankudinov, S. N. Yannopoulos, and K. S. Andrikopoulos, J. Phys.: Condens. Matter **16**, S5103 (2004).

[11] A. V. Kolobov, P. Fons, A. I. Frenkel, A. L. Ankudinov, J. Tominaga, and T. Uruga, Nat. Mater. **3**, 703 (2004).

[12] S. Kohara, K. Kato, S. Kimura, H. Tanaka, T. Usuki, K. Suzuya, H. Tanaka, Y. Moritomo, T. Matsunaga, N. Yamada, Y. Tanaka,

H. Suematsu, and M. Takata, Appl. Phys. Lett. **89**, 201910 (2006).

[13] D. A. Baker, M. A. Paesler, G. Lucovsky, S. C. Agarwal, and P. C. Taylor, Phys. Rev. Lett. **96**, 255501 (2006).

[14] J.-J. Kim, K. Kobayashi, E. Ikenaga, M. Kobata, S. Ueda, T. Matsunaga, K. Kifune, R. Kojima, and N. Yamada, Phys. Rev. B **76**, 115124 (2007).

[15] J. Akola and R. O. Jones, Phys. Rev. B **76**, 235201 (2007).

[16] J. Akola and R. O. Jones, J. Phys.: Condens. Matter **20**, 465103 (2008).

[17] S. Caravati, M. Bernasconi, T. D. Kühne, M. Krack, and M. Parrinello, Appl. Phys. Lett. **91**, 171906 (2007).

[18] J. Hegedüs and S. R. Elliott, Nat. Mater. **7**, 399 (2008).

[19] J. Akola and R. O. Jones, Phys. Rev. Lett. **100**, 205502 (2008).

[20] See, for example, D. Hohl and R. O. Jones, Phys. Rev. B **43**, 3856 (1991); X. Zhang and D. A. Drabold, Phys. Rev. Lett. **83**, 5042 (1999) (both amorphous Se); R. O. Jones and P. Ballone, J. Chem. Phys. **118**, 9257 (2003) (S_n clusters to $n=18$); L. Giacomazzi, C. Massobrio, and A. Pasquarello, Phys. Rev. B **75**, 174207 (2007) [$GeSe_2$].

[21] CPMD V3.12, Copyright IBM Corp. 1990–2008, Copyright MPI für Festkörperforschung Stuttgart, 1997–2001 (http://www.cpmd.org).

[22] J. P. Perdew, A. Ruzsinszky, G. I. Csonka, O. A. Vydrov, G. E. Scuseria, L. A. Constantin, X. Zhou, and K. Burke, Phys. Rev. Lett. **100**, 136406 (2008).

[23] J. P. Perdew, K. Burke, and M. Ernzerhof, Phys. Rev. Lett. **77**, 3865 (1996).

[24] N. Troullier and J. L. Martins, Phys. Rev. B **43**, 1993 (1991); the valence configurations are $4s^24p^2$(Ge), $5s^25p^3$(Sb), and $5s^25p^4$(Te), and the scalar-relativistic pseudopotentials contain nonlinear core corrections.

[25] The convergence of the plane-wave expansion has been tested on numerous small molecules, for many of which experimental structures are available. A cutoff of 15 Ry is adequate for these elements; 20 Ry is very good.

[26] G. J. Martyna, M. L. Klein, and M. Tuckerman, J. Chem. Phys. **97**, 2635 (1992); the chain modification of the Nosé-Hoover approach leads to a canonical ensemble even in nonergodic systems.

[27] The density of ℓ-GST-8,2,11 ($x=\frac{1}{9}$) is assumed to be that of ℓ-GeTe ($x=0$, T. Tsuchiya, private communication).

[28] D. Wamwangi, W. K. Njoroge, and M. Wuttig, Thin Solid Films **408**, 310 (2002); this value was measured for amorphous $Ge_4Sb_1Te_5$ (GST-8,2,10) and is very close to the density of a-GeTe.

[29] This cell was based on the crystalline structure of GST-225. See, for example, T. Matsunaga and N. Yamada, Phys. Rev. B **69**, 104111 (2004) and references therein. Very recent measurements on GST-8,2,11 (Ref. 4) give very similar values.

[30] See EPAPS Document No, E-PRBMDO-79-072913 for calcuated structure factors, pair distribution functions for cavities, projected densities of states, and effective charge distributions. For more information on EPAPS, see http://www.aip.org/pubservs/epaps.html.

[31] Ge atoms are denoted "tetrahedral" if all four bond distances are less than 3.0 Å (short bonds) and the average deviation of bond angles from the octahedral values exceeds 10°.

[32] W. Welnic, S. Botti, L. Reining, and M. Wuttig, Phys. Rev. Lett. **98**, 236403 (2007).

[33] V. M. Glazov, S. N. Chizhevskaya, and N. N. Glagoleva, *Liquid Semiconductors* (Plenum, New York, 1969).

[34] C. Bichara, M. Johnson, and J. P. Gaspard, Phys. Rev. B **75**, 060201(R) (2007).